JOC The Journal of Organic Chemistry

Article

pubs.acs.org/joc

# Synthesis, Physical Properties, and Light-Emitting Diode Performance of Phenazine-Based Derivatives with Three, Five, and Nine Fused Six-Membered Rings

Pei-Yang Gu,[†] Yongbiao Zhao,[‡] Jing-Hui He,[§] Jing Zhang,[†] Chengyuan Wang,[†] Qing-Feng Xu,[§] Jian-Mei Lu,[§] Xiao Wei Sun,*[,‡] and Qichun Zhang*[,†,∥]

[†]School of Materials Science and Engineering and [‡]School of Electrical and Electronic Engineering, Nanyang Technological University, Singapore 639798, Singapore

[§]College of Chemistry, Chemical Engineering and Materials Science, Soochow University, Suzhou, 215123, People's Republic of China

[∥]Division of Chemistry and Biological Chemistry, School of Physical and Mathematical Sciences, Nanyang Technological University, Singapore 637371, Singapore

Supporting Information

**ABSTRACT:** Realizing the control of emission colors of single molecules is very important in the development of full-color emitting materials. Herein, three novel phenazine derivatives (2,3,7,8-tetrakis(decyloxy)phenazine (**2a**), 2,3-didecyloxy-5,14-diaza-7,12-dioxo-9,10- dicyanopentacene (**2b**), and 2,3,13,14-tetradecyloxy-5,11,16,22-tetraaza-7,9,18,20-tetraoxo-8,19-dicyanoenneacene (**2c**)) have been successfully synthesized and fully characterized. Compound **2c** can emit blue light in toluene solution (450 nm), green light in the powder/film state (502/562 nm), and red light in the **2c**/TFA state (610 nm). The OLED with **2c** emits a strong green light at a peak of 536 nm with a maximum luminance of the OLED of about 8600 cd $m^{-2}$, which indicates that **2c** could be a promising fluorescent dye for OLED applications.

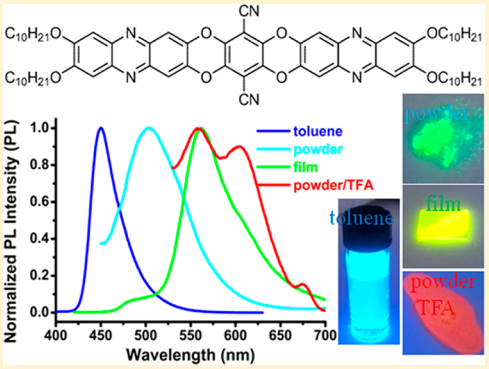


## INTRODUCTION

Conjugated organic molecules with multiple fused aromatic rings have attracted a great deal of interest from researchers due to their excellent performance in organic semiconductor devices.[1] Among these molecules, compounds with the "doping" of heteroatoms (using heteroatoms to replace CH groups in the conjugated frameworks) have received more attentions because the "doping" of heteroatoms could dramatically change the positions of the highest occupied molecular orbital (HOMO) and the lowest unoccupied molecular orbital (LUMO), the band gap, and the nature of charge transport.[2] In particular, azaacenes (using N atoms to replace CH group in conjugated backbones) have been demonstrated as promising active elements in organic field effect transistors (OFETs),[3] organic light-emitting diodes (OLEDs),[4] and organic memory devices.[5] However, most azaacenes have poor performances in OLEDs due to strong $\pi-\pi$ stacking and the formation of excimers in the solid state. On the other hand, the control of emission color is an important key factor in the development of full-color emitting materials.[6] Generally, the color control can be realized through modifying molecular structures with different substituent groups.[7] However, such modification is a complicated process and, in some cases, it is very difficult to realize full-color emission.[8] In addition to modification, another feasible approach to create full-color fluorescence is to tune the packing style of dye molecules, because the emission of organic solids is strongly dependent on their packing modes in the solid state.[9] Recently, the emission colors of organic dyes have been reasonably controlled through tuning environmental factors such as thermochromism,[10] piezochromism,[11] and acid-dependent[12] luminescence. These results make us believe that phenazine derivatives (one family member of azacenes) could be promising candidates to address this problem because: (1) phenazine units have been widely used as important color-changing cores for detection,[13] (2) phenazine groups can be easily protonated, which can change the electron-accepting ability,[14] and (3) introducing dioxin into molecular backbones might weaken $\pi-\pi$ stacking, which could enhance the luminescence.[15] In this report, three phenazine derivatives (2,3,7,8-tetrakis(decyloxy)phenazine (**2a**), 2,3-didecyloxy-5,14-diaza-7,12-dioxo-9,10-dicyanopentacene (**2b**), and 2,3,13,14-tetradecyloxy-5,11,16,22-tetraaza-7,9,18,20-tetraoxo-8,19- dicyanoenneacene (**2c**)) have been successfully synthesized and

**Received:** December 8, 2014
**Published:** March 3, 2015





DOI: 10.1021/jo5027707
J. Org. Chem. 2015, 80, 3030−3035

characterized. Their physical properties and their application in OLEDs were also investigated in detail.

## RESULTS AND DISCUSSION

**Synthesis of Phenazine Derivatives.** The synthetic procedures for phenazine compounds are described in Scheme 1. 7,8-Bis(decyloxy)phenazine-2,3-diol was synthesized according to a literature procedure,[5c] which could further react with 1-bromodecane (or 4,5-difluorophthalonitrile or tetrafluoroterephthalonitrile) to produce **2a** (or **2b**,**c**) in a high yield. The as-prepared compounds were confirmed by $^{1}$H NMR, $^{13}$C NMR, and mass spectroscopy. Strong efforts were made to grow suitable crystals of compounds **2a**–**c** for single-crystal analysis. Although compounds **2b**,**c** could form crystals, unfortunately, all as-obtained crystals were very thin and had very weak diffraction peaks (Supporting Information, Figure S17), which were unsuitable for data collection. This weak-diffraction problem might be caused by long alkyl chains.

**Scheme 1. Synthetic Route of 2a–c**[a]

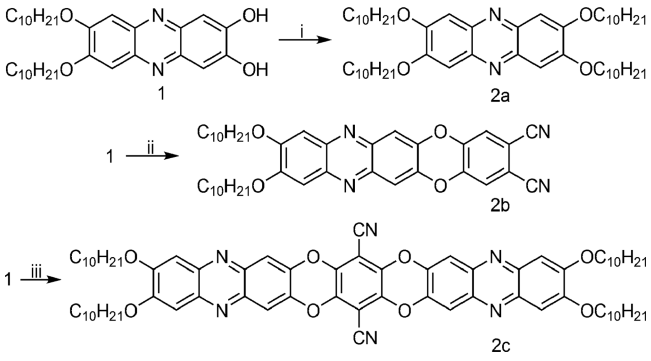


[a]Legend: (i) $K_2CO_3$, 1-bromodecane, DMF, $N_2$, 100 °C, 75%; (ii) $K_2CO_3$, 4,5-difluorophthalonitrile, DMF, $N_2$, 100 °C, 70%; (iii) $K_2CO_3$, tetrafluoroterephthalonitrile, DMF, $N_2$, 100 °C, 80%.

**Optical and Photoluminescent Properties.** The optical absorption spectra of compounds **2a**–**c** in toluene solution are shown in Figure 1, and the relevant parameters are summarized in Table 1. Compound **2a** has its maximum absorption at 404 nm, while **2b** possesses two prominent bands at 292 and 415 nm and **2c** has a band at 433 nm, which can be ascribed to a localized aromatic $\pi-\pi^*$ transition and phenazine core, respectively. The peak positions of the longest wavelengths of compounds **2a**–**c** have the trend **2a** < **2b** < **2c**, reflecting the impact of the conjugated degree on the electronic properties. Although the absorption of **2c** is not significantly influenced (only red-shifted 2 nm) by simply changing the solvent from toluene to chloroform (Figure 2), the protonation at the pyrazine unit of compound **2c** could cause a dramatic UV–visible absorption red shift (433 nm in toluene and 494 nm in trifluoroacetic acid (TFA)). The absorption edges of compounds **2a**–**c** extend to ~417, 430, and 450 nm, from which the optical band gaps ($E_g^{opt}$) are estimated to be 2.45, 2.38, and 2.27 eV, respectively.

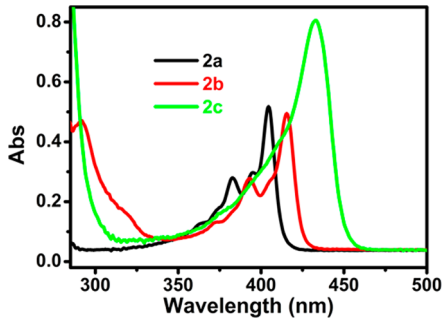


**Figure 1.** Absorption spectra of **2a**–**c** recorded in toluene solution ($10^{-5}$ mol $L^{-1}$).

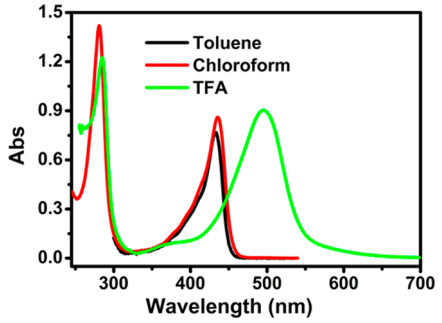


**Figure 2.** Absorption spectra of **2c** recorded in different solvents ($10^{-5}$ mol $L^{-1}$).

The photoluminescent (PL) behaviors of compounds **2a**–**c** in different solvents are shown in Figures 3 and 4 and Figures S13 and S14 (Supporting Information). The emission spectrum of compound **2c** displays only one peak at 450 nm, while the emission spectra of compounds **2a**,**b** show two peaks (408 and 432 nm for **2a** and 420 and 443 nm for **2b**), which may be due to the reabsorption of compounds **2a**,**b**. The PL wavelengths

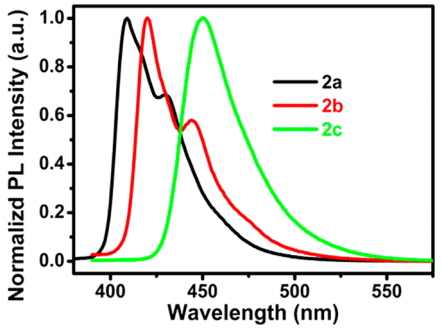


**Figure 3.** Normalized PL spectra of **2a**–**c** recorded in toluene solution.

**Table 1. Optical Data for Compounds 2a–c**

| | $\lambda_{abs}$, nm | | | $\lambda_{em}$, nm ($\varphi_F$, %) | | | | |
|---|---|---|---|---|---|---|---|---|
| dye | toluene | $CHCl_3$ | TFA | toluene | $CHCl_3$ | TFA | film | solid |
| **2a** | 404 | 265, 408 | 278, 527 | 408, 432 (13) | 422, 440 (46) | 575 (<1) | 452 | 453 |
| **2b** | 292, 415 | 291, 415 | 289, 473 | 420, 443 (15) | 427, 448 (24) | 511, 590 (<1) | 502 | 488 |
| **2c** | 433 | 281, 435 | 285, 494 | 450 (26) | 467 (32) | 547 (<1) | 562 | 502 |



DOI: 10.1021/jo5027707
J. Org. Chem. 2015, 80, 3030–3035

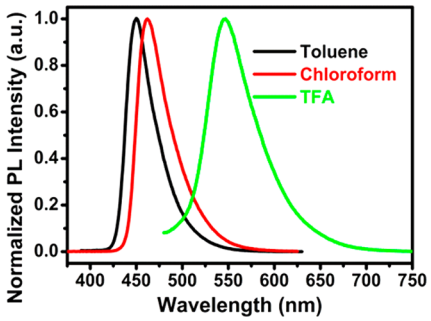


**Figure 4.** Normalized PL spectra of **2c** recorded in different solvents.

are red-shifted from **2a** to **2b** to **2c**, due to the increased conjugation degree. The emission wavelength of **2c** generally red-shifts about 17 nm from toluene to chloroform, but when toluene is replaced by TFA, the emission wavelength increases to 547 nm.

The emission behaviors of compounds **2a**−**c** in solid/film states have been studied, and the results are shown in Figures 5

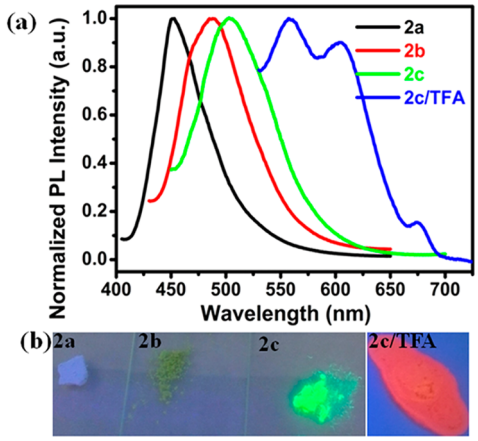


**Figure 5.** (a) Normalized PL spectra of solids **2a**−**c** and **2c**/TFA and (b) corresponding photographs under illumination by a 365 nm lamp.

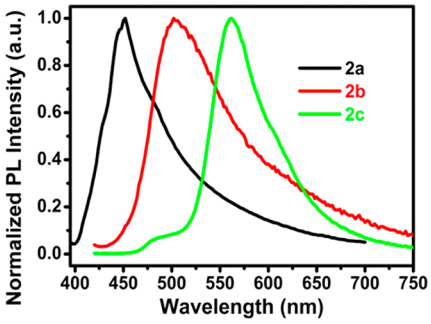


**Figure 6.** Normalized PL spectra of **2a**−**c** in thin film.

and 6. Typically, the emission wavelengths increased from **2a** (453 nm) to **2b** (488 nm) to **2c** (502 nm). The emission wavelength of the **2c**/TFA sample was red-shifted to 554 and 610 nm, while no emission was observed in **2a**/TFA and **2b**/TFA samples. The emission wavelengths of the three compounds in film states also increased from **2a** (452 nm) to **2b** (502 nm) to **2c** (562 nm). The emission wavelengths of compounds **2b**,**c** in powder and film states are different, which may be due to the different molecular packing structures.[16] As a result, compound **2c** can emit blue light in toluene solution (450 nm), green light in the powder/film state (502/562 nm), and red light in the **2c**/TFA state (610 nm).

**Thermal and Electrochemical Behavior.** The thermal properties of compounds **2a**−**c** were evaluated by TGA under a nitrogen atmosphere. As shown in Figure S15 (Supporting Information), the three compounds display very good thermal stability with onset decomposition temperatures of ∼337, 381, and 372 °C (considering the 5% weight loss temperature), respectively.

Cyclic voltammetry measurements of compounds **2a**−**c** were performed in dichloromethane solution (with 0.1 M $TBAPF_6$) to investigate the electrochemical properties. As shown in Figure 7, the onset oxidation potentials ($E_{ox}^{onset}$) of compounds

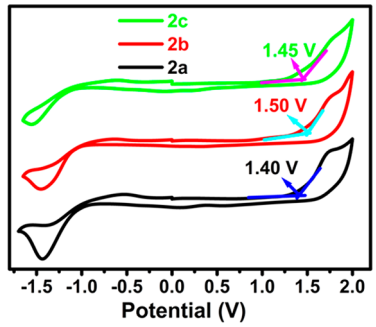


**Figure 7.** Cyclic voltammogram curves of compounds **2a**−**c** in dichloromethane solution with $TBAPF_6$ (0.1 M) as the supporting electrolyte. Scan rate: 100 mV $s^{-1}$.

**2a**−**c** are 1.40, 1.50, and 1.45 V, respectively. The HOMO energy levels of three compounds were estimated to be 5.98, 6.08, and 6.03 eV from the onset oxidation potential with reference to $Fc^+/Fc$ (−4.8 eV) using the equation $E_{HOMO} = -[4.8 - E_{Fc} + E_{ox}^{onset}]$ eV. The LUMO energy levels of three compounds are 3.53, 3.70, and 3.76 eV according to the equation $E_{LUMO} = E_{HOMO} + E_g^{opt}$.

**Theoretical Calculations.** To gain further insight into their electronic structure, theoretical calculations of compounds **2a**−**c** were performed using density functional theory (DFT) with the generalized gradient approximation (GGA), which is implemented in the DMol[3] code.[17] As shown in Figure 8, the HOMO and LUMO of **2a** are evenly distributed on the main conjugated backbone, suggesting a weak intramolecular charge

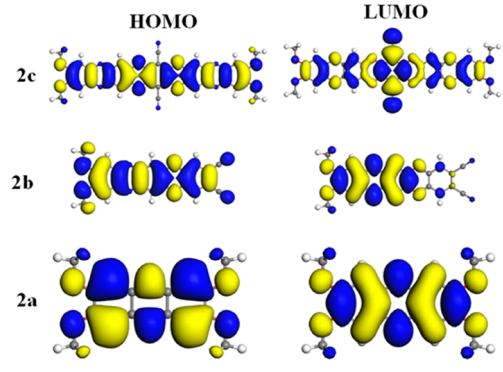


**Figure 8.** HOMO and LUMO levels of compounds **2a**−**c**. The isovalue to plot all orbital surfaces is 0.01 e/Å$^3$.



DOI: 10.1021/jo5027707
J. Org. Chem. 2015, 80, 3030−3035

transfer (ICT), resulting from the molecule's symmetric backbone as well as the lack of strongly electron withdrawing groups. In contrast, the electron density of the HOMO of **2b** is mainly located on the whole skeleton but the LUMO prefers to distribute on the phenazine group due to the existence of ending cyano groups. Similarly, on the basis of the electron densities for the HOMO and LUMO of **2c**, there is obvious ICT from the heteroacene backbone to the central electron-withdrawing cyano pairs (CN). Therefore, **2c** displays the largest red shift with an increased polarity of solvents. Among these compounds, compound **2a** possesses the highest energy band gap (2.45 eV) while **2b**,**c** have relatively smaller energy gaps (2.35 and 1.98 eV, respectively). The total order of energy band gaps is $\Delta E_1 > \Delta E_2 > \Delta E_3$, which is consistent with optical results. This result suggests that the band gaps could be tuned by varying the number of conjugated aromatic rings.

**Electroluminescent Characteristics.** On the basis of photophysical and electrochemical studies, compounds **2a**–**c** were further studied as active materials in OLEDs. The OLED devices were fabricated with a common structure of ITO/ZnO (40 nm)/emitter/CBP (50 nm)/$MoO_3$ (5 nm)/Al (200 nm), where the emitters are **2a**–**c**, respectively. As shown in Figure 9, the *J*–*V* curves of the three OLEDs are greatly different. The

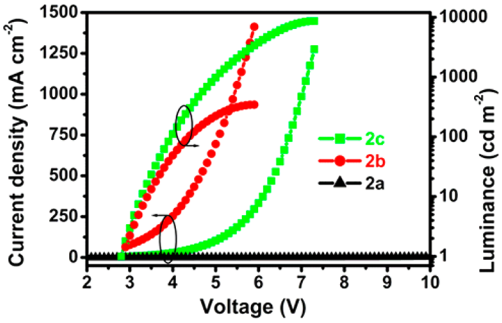


**Figure 9.** Current density vs voltage and luminance vs voltage characteristics for OLEDs with compounds **2a**–**c**. For **2a**, the device does not emit any light and only the current density–voltage curve is shown.

OLED with **2b** shows the highest current, and that with **2c** shows a moderate current, while that with **2a** shows a very low current. This indicates there might be substantial differences in the mobilities of the three compounds. The turn-on voltages for the OLEDs with **2b**,**c** are almost the same at 2.8 V. However, due to Pa LQY difference, the OLED with **2c** shows luminance much higher than that with **2b**. The maximum luminance of the OLED with **2c** is about 8600 cd m$^{-2}$, which indicates that **2c** is a promising fluorescent dye for OLED applications. As a comparison, the OLED with **2a** does not show any emission due to its poor charge carrier transport properties. The external quantum efficiency (EQE) curves for OLEDs with **2b**,**c** are shown in Figure 10. As expected, the OLED with **2c** shows a maximum EQE of 0.33%, which is much higher than that of the OLED with **2b** (maximum EQE of 0.014%). In this research, we are interested in understanding how oxygen atoms in the backbone of as-prepared compounds (compounds **2b**,**c**) affect PL emission and external quantum efficiency in devices. In fact, oxygen atoms in compounds **2b**,**c** can absorb photons that generate oxygen vacancies upon excitation, which is useful for PL emission. In other words, more benzodioxane units are introduced into the backbone of the molecules, leading to

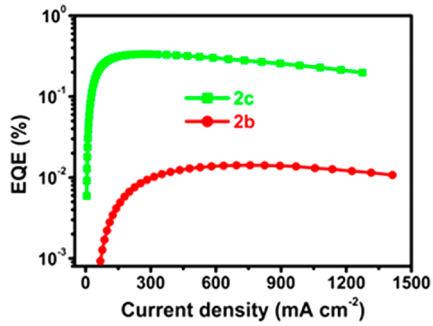


**Figure 10.** External quantum efficiency curves for OLEDs with compounds **2b**,**c**.

much stronger emission. As a result, the maximum luminance and external quantum efficiency of **2c** are better than those of **2a**,**b**. The electroluminance curves are shown in Figure 11. The

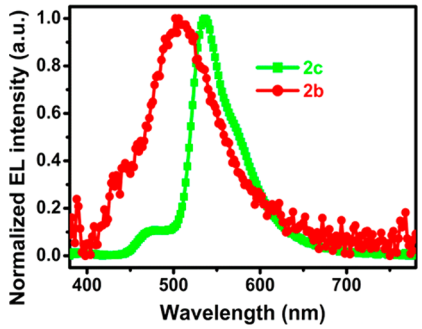


**Figure 11.** Normalized electroluminance curves for OLEDs with compounds **2b**,**c**.

OLED with **2c** emits at a peak of 536 nm with shoulder emissions at 472 nm owing to the different molecular packing, while for the OLED with **2b**, the emission peak shifts to 505 nm.

## CONCLUSIONS

In summary, we have successfully synthesized three phenazine-based derivatives with three, five, and nine fused aromatic rings for solution-processed OLEDs. Compound **2c** can emit blue light in toluene solution (450 nm), green light in the powder/film state (502/562 nm), and red light in the **2c**/TFA state (610 nm). The OLED with **2c** emits strong green light at a peak of 536 nm with a maximum luminance of the OLED of about 8600 cd m$^{-2}$, which indicates that **2c** is a promising fluorescent dye for OLED applications.

## EXPERIMENTAL SECTION

**Materials.** The species 10% Pd/C, hydrazine monohydrate, 4,5-difluorophthalonitrile, tetrafluoroterephthalonitrile, 2,5-dihydroxy-1,4-benzoquinone, and 1-bromodecane are commercially available. Other chemicals and solvents were used directly without further purification.

**Instrumentation and Characterization.** High-resolution mass spectra (HRMS) were recorded on a Q-Tof mass spectrometer. Cyclic voltammetry measurements were carried out on a electrochemical analyzer. Glassy carbon (diameter 1.6 mm; area 0.02 cm$^2$) was used as a working electrode, and platinum wires were used as a counter electrode and a reference electrode, respectively. $Fc^+/Fc$ was used as an internal standard. Potentials were recorded versus $Fc^+/Fc$ in a solution of anhydrous dichloronethane with 0.1 M tetrabutylammonium hexafluorophosphate ($TBAPF_6$) as a supporting electrolyte at a scan rate of 100 mV s$^{-1}$.



DOI: 10.1021/jo5027707
*J. Org. Chem.* 2015, 80, 3030–3035

**Fabrication of OLED Devices.** All devices were fabricated on commercial ITO-coated glass substrates (15 Ω/sq). The ITO substrates were treated in order by ultrasonic bath sonication of detergent, deionized water, acetone, and isopropyl alcohol, each with a 20 min interval. Then the ITO substrates were dried with nitrogen gas and baked in an oven at 80 °C for 30 min. Then, ZnO layers were grown by a spin-coating method.[18] The pretreated substrates were transferred into a glovebox, where the dye emitters were spin-coated at a rate of 2000 rpm from chloroform solution with a concentration of 5 mg $mL^{-1}$. Subsequently, the substrates were transferred into a thermal evaporator, where the organic, inorganic, and metal functional layers were grown layer by layer at a base pressure of less than $4 \times 10^{-4}$ Pa. The evaporation rates were monitored with several quartz crystal microbalances located above the crucibles and thermal boats. For organic semiconductors and metal oxides, the typical evaporation rates were about 0.1 nm $s^{-1}$, and for aluminum (Al), the evaporation rate was about 1−5 nm $s^{-1}$. The intersection of Al and ITO forms a 1 mm × 1 mm active device area. *J*−*V* and *L*−*V* data were collected with a source meter and a calibrated Si photodetector with a customized Labview program. The electroluminance spectrum was measured with a spectrometer.

**Syntheses.** *2,3,7,8-Tetrakis(decyloxy)phenazine (**2a**).* A mixture of 7,8-bis(decyloxy)phenazine-2,3-diol (524 mg, 1 mmol) and $K_2CO_3$ (552 mg, 4 mmol) in 5 mL of DMF was stirred for 1 h under a nitrogen atmosphere. 1-Bromodecane (664 mg, 3 mmol) was added to 2 mL of DMF, and the mixture was heated to 100 °C for 24 h. The mixture was cooled to ambient temperature before being poured into deionized water (200 mL). The obtained precipitate was isolated by filtration and washed with water. Further purification was effected by chromatography on silica gel using dichloromethane as eluent. A light yellow powder (600 mg, 0.75 mmol) was obtained in 75% yield. Mp: 134−136 °C. $^1$H NMR (300 MHz, $CDCl_3$): $\delta$ 7.32 (s, 4H), 4.22 (t, $J$ = 6.6 Hz, 8H), 2.01−1.88 (m, 8H), 1.60−1.50 (m, 16H), 1.43−1.30 (m, 40H), 0.90 (t, $J$ = 6.6 Hz, 12H). $^{13}$C NMR (400 MHz, $CDCl_3$): $\delta$ 152.9, 139.6, 105.7, 69.1, 31.9, 29.6, 29.6, 29.4, 29.3, 28.8, 26.0, 22.7, 14.1. HRMS (ESI): formula: $C_{52}H_{89}N_2O_4$; calcd, 805.6822; found, 805.6757.

*2,3-Didecyloxy-5,14-diaza-7,12-dioxo-9,10-dicyanopentacene (**2b**).* Compound **2b** was synthesized as a green powder in 70% yield from 7,8-bis(decyloxy)phenazine-2,3-diol and 4,5-difluorophthalonitrile by following the general procedure described for **2a**. Mp: 89−91 °C. $^1$H NMR (300 MHz, $CDCl_3$): $\delta$ 7.57 (s, 2H), 7.35 (s, 2H), 7.24 (s, 2H), 4.22 (t, $J$ = 6.6 Hz, 4H), 2.01−1.90 (m, 4H), 1.54 (dd, $J$ = 14.8, 7.0 Hz, 4H), 1.45−1.28 (m, 24H), 0.90 (t, $J$ = 6.6 Hz, 6H). $^{13}$C NMR (400 MHz, $CDCl_3$): $\delta$ 154.8, 144.3, 142.0, 141.5, 140.0, 121.8, 114.4, 113.1, 111.7, 105.3, 69.4, 31.9, 29.6, 29.6, 29.3, 28.7, 26.0, 22.7, 14.1. HRMS (ESI): formula, $C_{40}H_{49}N_4O_4$; calcd, 649.3754; found, 649.3799.

*2,3,13,14-Tetradecyloxy-5,11,16,22-tetraaza-7,9,18,20-tetraoxo-8,19-dicyanoenneacene (**2c**).* 7,8-Bis(decyloxy)phenazine-2,3-diol (524 mg, 1 mmol) and $K_2CO_3$ (690 mg, 5 mmol) were placed in a two-necked round-bottom flask under a nitrogen atmosphere. DMF (20 mL) was added. After the mixture was stirred for 1 h at room temperature, tetrafluoroterephthalonitrile (90 mg, 0.45 mmmol) was added and this mixture was heated to 100 °C for 3 days. The mixture was cooled to ambient temperature before being poured into deionized water (200 mL). Yellow crystals were obtained which were recrystallized from chloroform and dried under vacuum to give **2c** (470 mg, 0.8 mmol, yield 80%). Mp: 214−216 °C. $^1$H NMR (400 MHz, $CDCl_3$): $\delta$ 7.67 (s, 2H), 7.25 (s, 2H), 4.19 (t, $J$ = 6.5 Hz, 4H), 1.97−1.89 (m, 4H), 1.68−1.46 (m, 8H), 1.44−1.22 (m, 24H), 0.89 (t, $J$ = 6.6 Hz, 6H). $^{13}$C NMR (400 MHz, $CDCl_3$): $\delta$ 154.8, 141.9, 140.5, 139.7, 137.9, 113.4, 108.6, 105.2, 94.7, 69.4, 31.9, 29.6, 29.6, 29.4, 29.4, 28.8, 26.0, 22.7, 14.1. MS (ESI, the isotopomer with two $^{15}$N atoms): formula, $C_{72}H_{93}N_6O_8$; calcd, 1171.70; found, 1171.68. Anal. Calcd for $C_{72}H_{92}N_6O_8$: C, 73.94; H, 7.93; N, 7.19. Found: C, 73.72; H, 7.97; N, 7.16.

## ■ ASSOCIATED CONTENT

### Ⓢ Supporting Information

Text giving general information and figures giving the original TGA, $^1$H NMR, $^{13}$C NMR, HR-MS, absorption, and emission spectra. This material is available free of charge via the Internet at http://pubs.acs.org.

## ■ AUTHOR INFORMATION


### Corresponding Authors

*E-mail for X.W.S.: Exwsun@ntu.edu.sg.

*E-mail for Q.Z.: qczhang@ntu.edu.sg.


### Notes

The authors declare no competing financial interest.

## ■ ACKNOWLEDGMENTS

Q.Z. acknowledges financial support from the AcRF Tier 1 (RG 16/12 and RG 133/14) and Tier 2 (ARC 20/12 and ARC 2/13) from the MOE and the CREATE program (Nanomaterials for Energy and Water Management) from the NRF.

## ■ REFERENCES


(1) (a) Kotwica, K.; Bujak, P.; Wamil, D.; Materna, M.; Skorka, L.; Gunka, P. A.; Nowakowski, R.; Golec, B.; Luszczynska, B.; Zagorska, M.; Pron, A. *Chem. Commun.* **2014**, *50*, 11543. (b) Li, J.; Yan, F.; Gao, J.; Li, P.; Xiong, W.-W.; Zhao, Y.; Sun, X. W.; Zhang, Q. *Dyes Pigm.* **2015**, *112*, 93. (c) Xiao, C.; Jiang, W.; Li, X.; Hao, L.; Liu, C.; Wang, Z. *ACS Appl. Mater. Interfaces* **2014**, *6*, 18098. (d) Ward, J. W.; Li, R.; Obaid, A.; Payne, M. M.; Smilgies, D.-M.; Anthony, J. E.; Amassian, A.; Jurchescu, O. D. *Adv. Funct. Mater.* **2014**, *24*, 5052. (e) Kim, C. H.; Hlaing, H.; Payne, M. M.; Yager, K. G.; Bonnassieux, Y.; Horowitz, G.; Anthony, J. E.; Kymissis, I. *ChemPhysChem* **2014**, *15*, 2913. (f) Xiao, J.; Yang, B.; Wong, J. I.; Liu, Y.; Wei, F.; Tan, K. J.; Teng, X.; Wu, Y.; Huang, L.; Kloc, C.; Boey, F.; Ma, J.; Zhang, H.; Yang, H.; Zhang, Q. *Org. Lett.* **2011**, *13*, 3004. (g) Zhao, J.; Wong, J. I.; Wang, C.; Gao, J.; Ng, V. Z. Y.; Yang, H. Y.; Loo, S. C. J.; Zhang, Q. *Chem. - Asian J.* **2013**, *8*, 665. (h) Li, J.; Zhang, Q. *Synlett* **2013**, *24*, 686.

(2) (a) More, S.; Bhosale, R.; Mateo-Alonso, A. *Chem. - Eur. J.* **2014**, *20*, 10626. (b) Mateo-Alonso, A. *Chem. Soc. Rev.* **2014**, *43*, 6311. (c) Robins, K. A.; Jang, K.; Cao, B.; Lee, D. C. *Phys. Chem. Chem. Phys.* **2010**, *12*, 12727. (d) Lee, D.-C.; Jang, K.; McGrath, K. K.; Uy, R.; Robins, K. A.; Hatchett, D. W. *Chem. Mater.* **2008**, *20*, 3688. (e) Bunz, U. H.; Engelhart, J. U.; Lindner, B. D.; Schaffroth, M. *Angew. Chem., Int. Ed.* **2013**, *52*, 3810. (f) Zhang, Q.; Xiao, J.; Yin, Z. Y.; Duong, H. M.; Qiao, F.; Boey, F.; Hu, X.; Zhang, H.; Wudl, F. *Chem. Asian. J.* **2011**, *6*, 856. (g) Li, G.; Duong, H. M.; Zhang, Z.; Xiao, J.; Liu, L.; Zhao, Y.; Zhang, H.; Huo, F.; Li, S.; Ma, J.; Wudl, F.; Zhang, Q. *Chem. Commun.* **2012**, *48*, 5974. (h) Li, J.; Gao, J.; Li, G.; Xiong, W.; Zhang, Q. *J. Org. Chem.* **2013**, *78*, 12760.

(3) (a) Richards, G. J.; Hill, J. P.; Mori, T.; Ariga, K. *Org. Biomol. Chem.* **2011**, *9*, 5005. (b) He, Z.; Liu, D.; Mao, R.; Tang, Q.; Miao, Q. *Org. Lett.* **2012**, *14*, 1050. (c) Liang, Z.; Tang, Q.; Xu, J.; Miao, Q. *Adv. Mater.* **2011**, *23*, 1535. (d) Wu, Y.; Yin, Z.; Xiao, J.; Liu, Y.; Wei, F.; Tan, K. J.; Kloc, C.; Huang, L.; Yan, Q.; Hu, F.; Zhang, H.; Zhang, Q. *ACS Appl. Mater. Interfaces* **2012**, *4*, 1883. (e) Li, G.; Zheng, K.; Wang, C.; Leck, K. S.; Hu, F.; Sun, X. W.; Zhang, Q. *ACS Appl. Mater. Interfaces* **2013**, *5*, 6458.

(4) (a) Xu, X.; Yu, G.; Chen, S.; Di, C. A.; Liu, Y. *J. Mater. Chem.* **2008**, *18*, 299. (b) Nakayama, K.-i.; Hashimoto, Y.; Sasabe, H.; Pu, Y.-J.; Yokoyama, M.; Kido, J. *Jpn. J. Appl. Phys.* **2010**, *49*, 01AB11. (c) Fu, C.; Li, M.; Su, Z.; Hong, Z.; Li, W.; Li, B. *Appl. Phys. Lett.* **2006**, *88*, 093507.

(5) (a) Wang, C.; Wang, J.; Li, P. Z.; Gao, J.; Tan, S. Y.; Xiong, W. W.; Hu, B.; Lee, P. S.; Zhao, Y.; Zhang, Q. *Chem.—Asian J.* **2014**, *9*, 779. (b) Gu, P. Y.; Zhou, F.; Gao, J.; Li, G.; Wang, C.; Xu, Q. F.; Zhang, Q.; Lu, J. M. *J. Am. Chem. Soc.* **2013**, *135*, 14086. (c) Gu, P.-Y.; Gao, J.; Lu, C.-J.; Chen, W.; Wang, C.; Li, G.; Zhou, F.; Xu, Q.-F.; Lu,




DOI: 10.1021/jo5027707
*J. Org. Chem.* 2015, 80, 3030−3035

J.-M.; Zhang, Q. *Mater. Horiz.* **2014**, *1*, 446. (d) Wang, C.; Hu, B.; Wang, J.; Gao, J.; Li, G.; Xiong, W.-W.; Zou, B.; Suzuki, M.; Aratani, N.; Yamada, H.; Huo, F.; Lee, P. S.; Zhang, Q. *Chem. - Asian J.* **2015**, *10*, 116.

(6) (a) Nagata, Y.; Takagi, K.; Suginome, M. *J. Am. Chem. Soc.* **2014**, *136*, 9858. (b) Kwon, J. E.; Park, S.; Park, S. Y. *J. Am. Chem. Soc.* **2013**, *135*, 11239.

(7) (a) Guo, Z.-H.; Lei, T.; Jin, Z.-X.; Wang, J.-Y.; Pei, J. *Org. Lett.* **2013**, *15*, 3530. (b) Su, D.; Oh, J.; Lee, S.-C.; Lim, J. M.; Sahu, S.; Yu, X.; Kim, D.; Chang, Y.-T. *Chem. Sci.* **2014**, *5*, 4812.

(8) Goel, A.; Sharma, A.; Rawat, M.; Anand, R. S.; Kant, R. *J. Org. Chem.* **2014**, *79*, 10873.

(9) (a) Yang, Q. Y.; Lehn, J. M. *Angew. Chem., Int. Ed.* **2014**, *53*, 4572. (b) Li, R.; Xiao, S.; Li, Y.; Lin, Q.; Zhang, R.; Zhao, J.; Yang, C.; Zou, K.; Li, D.; Yi, T. *Chem. Sci.* **2014**, *5*, 3922. (c) Cheng, X.; Li, D.; Zhang, Z.; Zhang, H.; Wang, Y. *Org. Lett.* **2014**, *16*, 880.

(10) (a) Liu, X.; Li, S.; Feng, J.; Li, Y.; Yang, G. *Chem. Commun.* **2014**, *50*, 2778. (b) Guo, Y.; Gu, S.; Feng, X.; Wang, J.; Li, H.; Han, T.; Dong, Y.; Jiang, X.; James, T. D.; Wang, B. *Chem. Sci.* **2014**, *5*, 4388.

(11) (a) Metz, A. E.; Podlesny, E. E.; Carroll, P. J.; Klinghoffer, A. N.; Kozlowski, M. C. *J. Am. Chem. Soc.* **2014**, *136*, 10601. (b) Pawle, R. H.; Haas, T. E.; Muller, P.; Thomas, S. W., III *Chem. Sci.* **2014**, *5*, 4184.

(12) (a) Wang, K.; Huang, S.; Zhang, Y.; Zhao, S.; Zhang, H.; Wang, Y. *Chem. Sci.* **2013**, *4*, 3288. (b) Liu, D.; Zhang, Z.; Zhang, H.; Wang, Y. *Chem. Commun.* **2013**, *49*, 10001. (c) Amir, E.; Murai, M.; Amir, R. J.; Cowart, J. S.; Chabinyc, M. L.; Hawker, C. J. *Chem. Sci.* **2014**, *5*, 4483.

(13) Laursen, J. B.; Nielsen, J. *Chem. Rev.* **2004**, *104*, 1663.

(14) (a) Singh, P.; Baheti, A.; Thomas, K. R. *J. Org. Chem.* **2011**, *76*, 6134. (b) Bunz, U. H. *Chem. - Eur. J.* **2009**, *15*, 6780. (c) Ye, Q.; Chang, J.; Shao, J.; Chi, C. *J. Mater. Chem.* **2012**, *22*, 13180.

(15) (a) McKeown, N. B.; Budd, P. M. *Chem. Soc. Rev.* **2006**, *35*, 675. (b) Chen, S.; Yi, W.; Duhamel, J.; Heinrich, K.; Bengtson, G.; Fritsch, D. *J. Phys. Chem. B* **2013**, *117*, 5249.

(16) (a) McGrath, K. K.; Jang, K.; Robins, K. A.; Lee, D. C. *Chem. - Eur. J.* **2009**, *15*, 4070. (b) Jang, K.; Brownell, L. V.; Forster, P. M.; Lee, D. C. *Langmuir* **2011**, *27*, 14615.

(17) (a) Delley, B. *J. Chem. Phys.* **2000**, *113*, 7756. (b) Zhou, F.; He, J.-H.; Liu, Q.; Gu, P.-Y.; Li, H.; Xu, G.-Q.; Xu, Q.-F.; Lu, J.-M. *J. Mater. Chem. C* **2014**, *2*, 7674.

(18) Hofle, S.; Schienle, A.; Bruns, M.; Lemmer, U.; Colsmann, A. *Adv. Mater.* **2014**, *26*, 2750.



DOI: 10.1021/jo5027707
*J. Org. Chem.* 2015, 80, 3030−3035